Brain Research 1742 (2020) 146890

Contents lists available at ScienceDirect

Brain Research

journal homepage: www.elsevier.com/locate/brainres

Research report

Individual differences in white and grey matter structure associated with verbal habits of thought

Justin C. Hayes[a,b], Katherine L. Alfred[a,b,*,1], Rachel G. Pizzie[a,b,c], Joshua S. Cetron[a,d], David J.M. Kraemer[a]

[a] Department of Education Dartmouth College, 6103 Winifred Raven House Hanover, NH 03755, United States
[b] Department of Psychological and Brain Sciences, Dartmouth College 6207 Moore Hall Hanover, NH 03755, United States
[c] Department of Psychology, Georgetown University 305 White-Gravenor Hall 3700 O Street NW Washington, DC 20057, United States
[d] Department of Psychology, Harvard University William James Hall 33 Kirkland Street Cambridge, MA 02138, United States

HIGHLIGHTS

- Individuals differ in the degree that they attend to visual and verbal information.
- Word bias is associated with volumetric differences in grey and white matter.
- Word bias is linked to greater myelination of fibers in speech production network.

ARTICLE INFO

Keywords:
Individual differences
Diffusion tensor imaging
Morphometry
Attention

ABSTRACT

Modality specific encoding habits account for a significant portion of individual differences reflected in functional activation during cognitive processing. Yet, little is known about how these *habits of thought* influence long-term structural changes in the brain. Traditionally, habits of thought have been assessed using self-report questionnaires such as the visualizer-verbalizer questionnaire. Here, rather than relying on subjective reports, we measured habits of thought using a novel behavioral task assessing attentional biases toward picture and word stimuli. Hypothesizing that verbal habits of thought are reflected in the structural integrity of white matter tracts and cortical regions of interest, we used diffusion tensor imaging and volumetric analyses to assess this prediction. Using a whole-brain approach, we show that word bias is associated with increased volume in several bilateral language regions, in both white and grey matter parcels. Additionally, connectivity within white matter tracts within an *a priori* speech production network increased as a function of word bias. These results demonstrate long-term structural and morphological differences associated with verbal habits of thought.

1. Introduction

As students sit in a lecture, processing the information conveyed by their professors, they create an internal representation of that information—for some it is a list of key words; for others it is a mental image or diagram. Over time, people develop *habits of thought* (HTs)—consistent neurocognitive habits of encoding and retrieving information. These habits comprise a global cognitive framework directing low-level information processing strategies (Messick et al., 1976). Such habits vary along a modality-specific continuum, with individuals consistently using a verbal or visuospatial strategy (Blazhenkova & Kozhevnikov, 2009). Presumably, visualizers encode conceptual information pictorially or spatially, while verbalizers encode information linguistically or phonologically. Yet, little is known about the long-term neural consequences of favoring one strategy over another.

Recently, a number of neuroimaging studies (Alfred et al., 2019; Kraemer et al., 2009; Miller et al., 2009) used fMRI to identify task-specific functional markers associated with HTs. Miller and colleagues (2009, 2012) demonstrated the consistency of individuals' task-related BOLD activation across retrieval tasks assessing episodic, working, and semantic memory. The activation was remarkably similar within, but not between, individuals when compared across all three memory tasks and also across time. Additionally, HTs—assessed as cognitive styles

* Corresponding author.
E-mail address: katherine.l.alfred.gr@dartmouth.edu (K.L. Alfred).
[1] Indicates co-first author.

https://doi.org/10.1016/j.brainres.2020.146890
Received 7 May 2020; Accepted 12 May 2020
Available online 19 May 2020
0006-8993/

and task-specific strategies—account for a significant proportion of the variance associated with individuals' unique patterns of activation while performing memory tasks (Hsu et al., 2011; Kirchhoff & Buckner, 2006; Kraemer et al., 2009; Miller et al., 2012). These results suggest that individuals rely on stable, idiosyncratic neural processing networks, subsuming brain regions underlying their customary modality of information processing, when encoding and retrieving information.

Consistent with the idea that HTs lead to the formation of stable neural networks, recent work demonstrates task-specific functional activation in modality congruent regions of cortex (verbal or visual) when assessing individual differences associated with HTs. For instance, Kraemer, Hamilton, Messing, Desantis, & Thompson-Schill, 2014 used repetitive transcranial magnetic stimulation (rTMS) to disrupt the ability of individuals habitually relying on a verbal information processing strategy (i.e. *verbalizers*) to convert visual information into a verbal modality. The authors targeted a functionally defined region within the left supramarginal gyrus (SMG), a cortical region previously shown to be active while verbalizers process nameable pictures (Kraemer et al., 2009). Consistent with the "Conversion Hypothesis"—i.e., verbalizers translate pictorial information into linguistic representations, and vice versa—disrupting this region with rTMS pulses made it more difficult for verbalizers to label nameable objects. Furthermore, the amount of disruption caused by rTMS followed a gradient associated with self-reported verbal scores on an assessment measuring HTs—in other words, high verbalizers' performance was disrupted more than moderate verbalizers whose performance was disrupted more than low verbalizers. Recently, Alfred and colleagues (2019) found convergent results, demonstrating that individuals with an attentional bias toward verbal information relied on left hemisphere perisylvian regions, including SMG, when retrieving domain general semantic information. In other words, regardless of whether items were presented as words or pictures, verbalizers relied on a verbal network while retrieving them. Taken together, these results suggest that verbalizers use their preferred modality of processing regardless of the format in which a stimulus is presented, and that such HTs are reflected by activation in predictable brain regions, consistent across studies. That such studies show convergence across time suggests the presence of stable networks varying as a function of HTs.

Repeatedly activating modality specific cortical regions when encoding and retrieving information results in enhanced connectivity within those regions. For instance, Sahyoun and colleagues (2010a,b) show that individuals with an ASD diagnosis who favor visuospatial processing show enhanced myelination of white matter within regions of posterior visual cortex. Diffusion tensor imaging (DTI; for a review see Soares et al., 2013) provides information about network stability and connectivity. As such, DTI has been used to elucidate unique connectivity profiles for individuals with clinical diagnoses, including autism spectrum disorder (ASD; Sahyoun and colleagues, 2010a,b), multiple sclerosis (MS; e.g. Lowe et al., 2008), Parkinson's disease (PD; for a review see Tessitore et al., 2016), and schizophrenia (for a review see Kubicki et al., 2007). Here, we demonstrate that methods previously used to study clinical populations can be applied to neurotypical populations, differentiating among individuals as a function of verbal HTs.

In the current study, we hypothesized that verbal HTs would be reflected by structural and morphological distinctions within the brain, indicating the degree to which individuals habitually encode and retrieve information in a linguistic modality, as measured by an attentional bias task. In a whole-brain analysis, we compared volumetric data found within grey and white matter parcels, as defined within a commonly referenced brain atlas, with the results of the AB task. Constraining our search to an *a priori* speech production network, we also used diffusion tensor imaging (DTI) to elucidate patterns of neural connectivity indicative of persistent HTs within regions associated with phonological and speech processing.

2. Method

2.1. Participants

Twenty-nine (16 female, M_{AGE} = 20.7 years) undergraduate and graduate students attending Dartmouth College participated in the experiment. All participants were right-handed, native English speakers with normal or corrected-to-normal vision. No participants reported having a history of neurological or psychiatric disorders. In addition, in accordance with Dartmouth's Committee for the Protection of Human Subjects (CPHS), all participants provided informed consent and received compensation, either cash or course credit, for their participation. One participant was omitted from our analyses due to incomplete data.

2.1.1. Attentional bias task

We used a novel, in-house task to assess HTs. This attentional bias task assessed the degree to which participants selectively attended to visual or verbal stimuli when required to report the identity of concurrently presented, incongruent pairs of line drawings and words. Importantly, participants were unaware that some trials would include incongruent stimuli. Participants were briefly (500 ms) presented with picture/word pairs of suits associated with playing cards (club, heart, spade), and instructed to report, as quickly as possible, the identity of the pair by pressing a key corresponding to one of three suits (J = club, K = heart, L = spade; Fig. 1**A**). Thus, a participant's attentional bias score was reflected by the percentage of target (incongruent) trials in which they pressed the key corresponding to either the word or picture (Fig. 1**B**). For 75% (1 4 4) of trials, the picture and word were congruent; for the remaining target trials (48), the picture and word were incongruent. Every object was presented during an equal number of trials. Additionally, the location of the word was counterbalanced such that it appeared above or below the picture with equal likelihood.

2.1.2. Image acquisition

Each subject was scanned on a 3 T Achieva Intera with a 32 channel SENSE birdcage head coil. We obtained T1-weighted anatomical images, capturing 160 continuous 1 mm sagittal slices with a high-resolution 3D rapid gradient echo sequence—TE = 4.6 ms; TR = 9.8 ms; FOV = 240 mm; flip angle = 8 degrees; voxel size = 1 0.94 0.94 mm. We collected diffusion weighted images using echoplanar imaging, capturing 70 continuous axial images 2 mm in thickness and 32 orthogonal diffusion gradients—TE = 91 ms; TR = 9013 ms; b value = 1000 s/mm2; FOV = 240 mm; flip angle = 90 degrees; voxel size = 1.875 1.875 2 mm.

2.1.3. Cognitive style and ability assessments

Participants completed a battery of behavioral assessments prior to being scanned. We used an automated, computerized version the Visualizer-Verbalizer Questionnaire (VVQ; Kirby et al., 1988) to assess cognitive style. The purpose of the scale is to assess the degree to which individuals preferentially process information verbally or visually. Participants reported how much they agreed or disagreed with a series of 20 statements using a 7-point likert scale ranging from 1 = strongly disagree to 7 = strongly agree—half of the items were reverse scored so that items assessing the verbal and visual dimensions of the scale were oriented in the same direction (e.g., high score = high verbal, low score = low verbal). Dream vividness items were omitted from the analysis given their tendency to interfere with the visuospatial dimension of the scale.

Participants completed two assessments designed to measure cognitive ability—the Automated Working Memory Assessment (AWMA; Alloway, 2007) and the Weschsler Abbreviated Scale of Intelligence (WASI; Wechsler, 1999). We used the AWMA to obtain verbal and visual working memory and the WASI to obtain verbal (Verbal Comprehension Index – VCI) and visual (Perceptual Reasoning Index – PRI) IQ

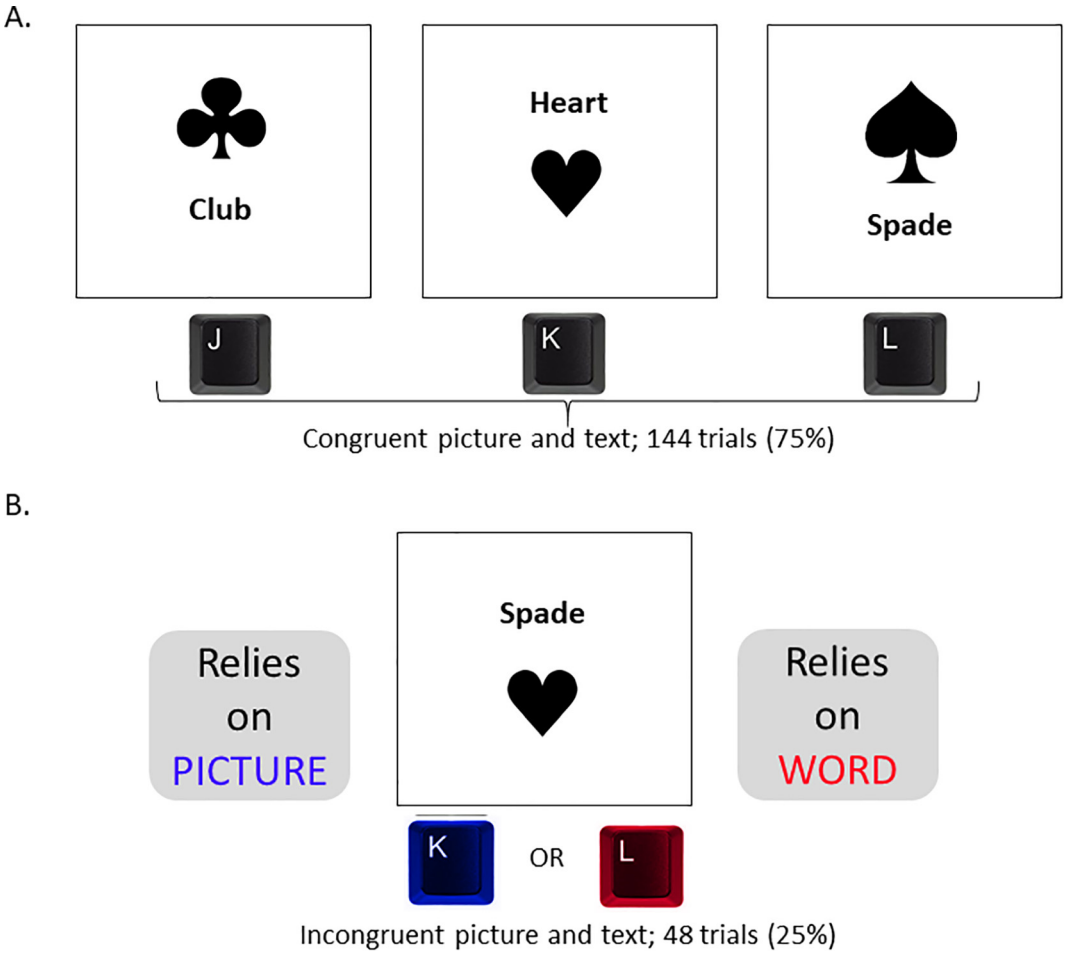

Fig. 1. Attentional bias task: A) Participants reported the identity of the object shown, pressing the J key if the object was a club, the K key if the object was a heart, or the L key if the object was a spade. For 75% of trials, the picture and word were congruent. B) For 25% of trials, the picture and word were incongruent. In this case, participants had to quickly decided whether to report the identity of either the picture or the word. In this figure, they would press the K key to report the picture of the heart, or the L key to report the word "Spade." Used with permission—Alfred et al., 2019.

scores.

2.1.4. Preprocessing diffusion weighted images

Voxelwise diffusion modeling was carried out using FMRIB's Diffusion Toolbox within FSL 5.0.10 (https://fsl.fmrib.ox.ac.uk/fsl/fslwiki; Smith et al., 2004). All images were eddy corrected before being used in further analysis. Diffusion weighted images were linearly aligned to the b = 0 image with 6 DOF. Fractional anisotropy (FA) values were determined by fitting tensors to the data, producing an estimation of the principal diffusion direction at every voxel. This estimation of diffusion parameters also models the crossing fibers within each voxel using a Gamma distribution to model the diffusion coefficient (see Jbabdi et al., 2012 for details).

2.1.5. Tract based spatial statistics

We used TBSS (Smith et al., 2006) to assess voxelwise integrity of WM DTI parameters at the whole-brain level. Every participant's FA image was non-linearly registered to the FMRIB58_FA image, producing a 4D file containing all FA files in standard (MNI152) space. Next, for each participant, the maximum FA value perpendicular to each voxel along the average center of tracts common to our sample, were aggregated. This produced a 4D, skeletonized image containing the FA values at the center of every major tract, as well as a skeletonized mean FA image representing the group average FA value at each location along the tracts. The mean FA image was thresholded at FA > 0.2 and the surviving voxels were used to produce a binarized skeleton mask. The GLM regressed participants' verbal bias scores—i.e. the percentage of time participants responded based on the identity of the word when picture/word pairs were incongruent—onto their FA values. The 4D skeletonized image, masked by the skeletonized FA mask, was then fed into FSL's Randomise (Winkler et al., 2014) algorithm for permutation-based, threshold-free cluster enhanced (TFCE; Smith & Nichols, 2009) voxelwise statistical analysis.

TFCE is an approach that is used to improve signal detection by using cluster-based thresholding instead of voxelwise thresholding without requiring the arbitrary selection of cluster thresholds. Specifically, TFCE utilizes the original raw statistical map and leverages that data to identify signal in spatially contiguous voxels, and then boosts that signal to the degree that there is similar signal in those spatially contiguous voxels. Importantly, TFCE has been shown to be a methodological improvement over traditional voxel and cluster thresholding techniques through the use of cluster-like voxelwise statistics and maintains detail from both of those levels (Smith & Nichols, 2009).

2.1.6. Extracting volumetric data

Participants' high-resolution T1-weighted brain images were used as input to Freesurfer (Fischl & Dale, 2000) to extract cortical and white-matter segmentations. We then extracted whole-brain volumetric (mm^3) data for both cortical (GM; 68 total, 34/hemisphere) and white matter parcels (68 total, 34/hemisphere) based on the Desikan-Killiany (DK) Atlas (Desikan et al., 2006). Finally, for each participant, every

grey matter and white matter parcel was divided by that participant's total brain volume, excluding ventricles, to control for individual differences in overall brain size.

2.2. Results

2.2.1. Do individuals differ in the degree to which their attention is biased toward verbal stimuli?

Habits of thought (visual/verbal) were assessed using an in-house task designed to detect attentional biases toward verbal stimuli. During incongruent trials, participants were presented conflicting verbal and visual information and had to choose whether to report the identity of the verbal or visual stimulus—a picture or word associated with playing card suits (club, heart, spade). We created a word bias score for each participant by computing the percentage of incongruent trials in which the identity of the word was reported. We chose to scale these scores such that a participant who responded only with the identities of the picture stimuli would have a word bias score of −1 and a participant who responded only with the identities of the word stimuli would have a word bias score of 1. By scaling in this way, a score of −0.8 and 0.8 would represent the same degree of bias in opposite directions, rather than scaling from 0 to 1, where participants with scores of 0.2 and 0.8 would be biased to the same degree in opposite directions but harder to interpret. Thus, each participant was given a single score, ranging from −1 to 1 (−1 = verbal stimuli never reported, 1 = verbal stimuli always reported). This score reflects the type of content participants were most likely to attend to, in addition to the degree to which they favored one type of information over the other—a high score (e.g., > 0.4) reflects a strong tendency to attend to verbal stimuli, a moderate score (e.g., ~ 0) reflects no bias toward visual or verbal stimuli, and a low score (e.g., < −0.4) reflects a strong tendency to attend to visual stimuli (see Fig. 2). Trials were discarded if participants reported a stimulus that was not on the screen (e.g., a club was reported if a participant saw a picture of a heart with the word "spade"). Overall, participants attended to pictures more than words (word $bias_{(M)}$ = -0.07) with 18 participants having a word bias of 0 or less (Fig. 2). However, there was a great deal of variation in the degree to which participants were biased toward pictures or words (word $bias_{(SD)}$ = 0.33).

Importantly, our attentional bias measure of habits of thought is able to measure variance in self-reported strategy selection better than self-reported measure of HTs, such as the VVQ for cognitive style. Specifically, one of the critical aspects of HTs is the process by which individuals convert material into their preferred format (e.g. converting pictures to words; demonstrated in Kraemer et al., 2009). In this study, that aspect is best captured by participant reporting of verbal strategies for visual content, such as the object pictures and abstract pictures. Our word attentional bias HT measure significantly correlated with reported use of verbal strategies in the object picture condition and the abstract picture condition ($r(26) = 0.38$, $p = 0.046$; $r(26) = 0.43$, $p = 0.022$). Further, the VVQ, a more traditional measure of HTs through cognitive styles, did not reliably or significantly correlate with the use of verbal strategies for visual content ($r(26) = -0.33$, $p = 0.086$ for object pictures; $r(26) = 0.29$, $p = 0.134$ for abstract pictures). This evidence supports our use of attentional bias to capture variance in HTs. Attentional bias therefore maintains the benefits of being a behavioral measure while still demonstrating a strong relationship with participant self-report measures of behavioral strategy.

2.2.2. Are structural differences associated with word bias reflected in brain morphology?

First, we tested the hypothesis that verbal HTs would be reflected by differences in grey matter morphology, by comparing volumetric data (participant T1-weighted brain images, see Method for further details) from cortical grey matter parcels with word bias scores using Pearson's correlations, including all 68 (34/hemisphere) cortical parcels included in the DKA. All correlations were adjusted for multiple comparisons using False Discovery Rate (FDR) correction (Benjamini & Hochberg, 1995). Across the whole brain three grey matter ROIs showed a significant relationship with performance on the word bias task (see Fig. 3), including two parcels in the left hemisphere: entorhinal cortex (LEC; $t(26) = 2.95$, $p < 0.01$, $r = 0.50$, [*95% CI*: 0.16 – 0.74]) and supramarginal cortex (LSMC; $t(26) = 2.06$, $p < 0.05$, $r = 0.37$, [*95% CI*: 0.001–0.37]), and one in the right hemisphere–temporal pole (RTP; $t(26) = 2.32$, $p < 0.05$, $r = 0.41$, [*95% CI*: 0.05 – 0.68]).

Next, we tested the hypothesis that verbal HTs would be reflected by differences in white matter morphology. We compared volumetric data (participant T1-weighted brain images, see Method for further details) taken from all 68 white matter parcels included in the DK atlas with word bias scores using Pearson's correlations, adjusting for multiple comparisons using FDR correction. Four parcels reached significance after FDR correction (see Fig. 4), all localized to the left hemisphere

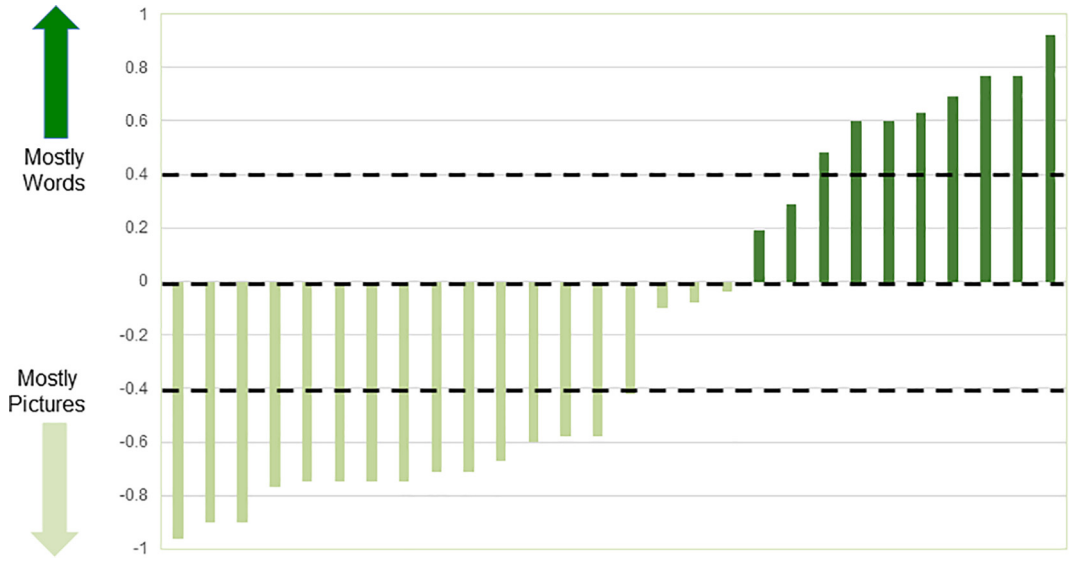

Fig. 2. Intersubject variability in word bias. The markers on the y-axis denote the percentage of target (incongruent) trials in which participants reported the word when presented with incongruent picture/word pairs. The dark green bars denote participants who reported the word on > 50% of trials. The light green bars denote participants who report the picture on > 50% of trials.

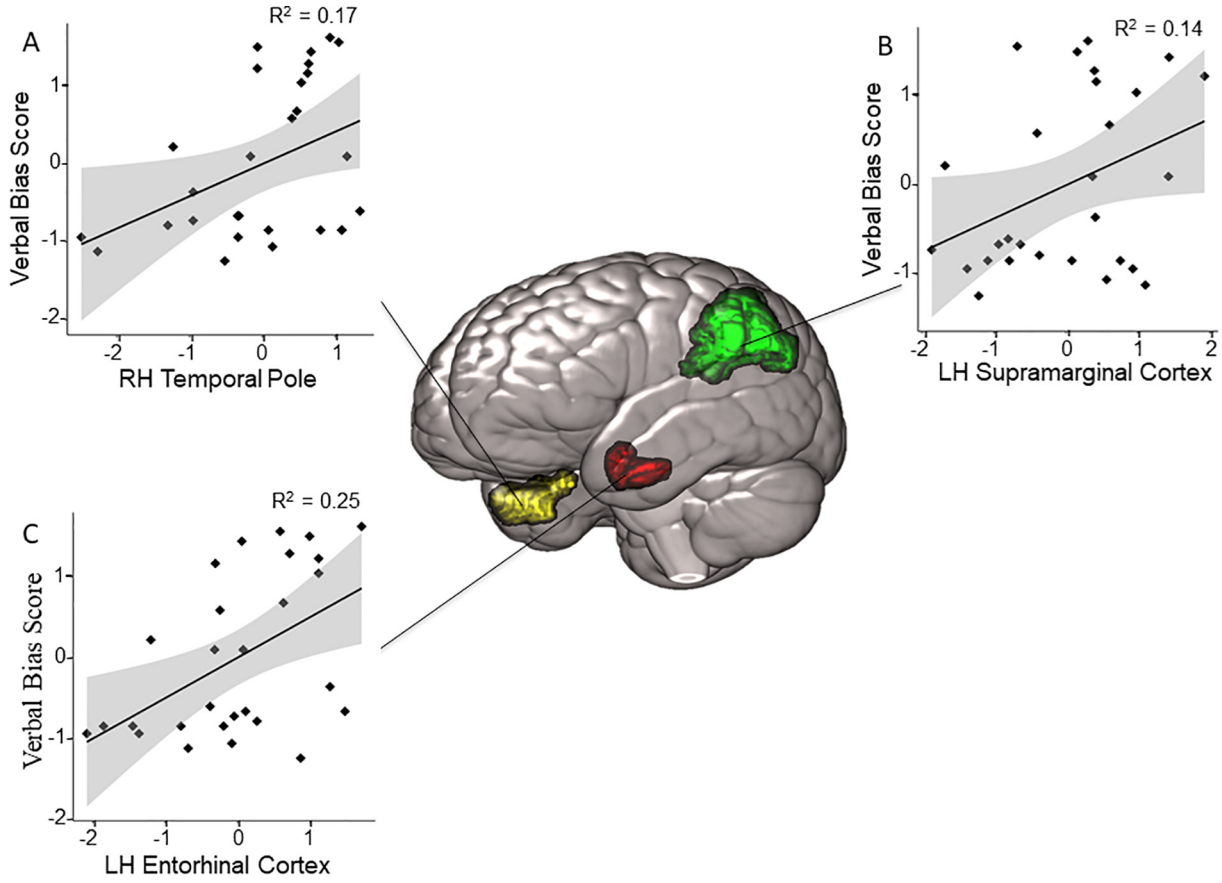

Fig. 3. Three grey matter volume parcels (Desikan-Killiany Atlas) positively correlate with word bias scores: A) right hemisphere temporal pole, B) left hemisphere supramarginal cortex, and C) left hemisphere entorhinal cortex. All data points were converted to z-values and Pearson's product-moment correlations are significant at the 0.05 alpha value after correcting for multiple comparisons (FDR).

(named after adjacent cortical structures), including: insular ($t(26) = 2.15$, $p = 0.04$, $r = 0.38$ [*95% CI*: 0.01–0.66]), rostral middle-frontal ($t(26) = 2.69$, $p < 0.05$, $r = 0.47$ [*95% CI*: 0.11–0.71]), parahippocampal ($t(26) = 2.05$, $p = 0.05$, $r = 0.37$ [*95% CI*: 0.0002–0.66]), and entorhinal ($t(26) = 3.34$, $p = 0.003$, $r = 0.55$ [*95% CI*: 0.22–0.76] volumes.

2.2.3. Are structural differences associated with word bias reflected in white matter integrity within an a priori defined speech production network?

As an independent analysis intended to obtain convergent evidence of structural differences associated with word bias scores, we ran a whole-brain GLM, regressing participants' word bias scores on fractional anisotropy (FA) values contained within a group-averaged white matter skeleton in standard space (MNI152_1mm). The model was thresholded at $p < 0.05$ after correcting for multiple comparisons (permutation testing; 1000 permutations) and threshold-free cluster enhancement (TFCE; Winkler et al., 2014). Cluster peaks were thresholded at $t > 2.3$ and clusters containing < 100 voxels were discarded from subsequent analyses. We then projected the surviving clusters onto a network from an automated *meta*-analysis of fMRI studies associated with the term "*speech production*" (SP; *NeuroSynth*; Yarkoni et al., 2011). The "speech production" *meta*-analytic map that was used is derived from nearly 15,000 studies, and the regions included are voxels that are *selectively* associated with the term "speech production" more than other terms. In other words, the *meta*-analytic map includes regions that are associated more with "speech production" than any other construct. The *meta*-analytic map is also FDR corrected, $p < 0.01$. Six clusters overlapped with the SP network. Table 1 summarizes these clusters, including the name of the major fiber tract, location in MNI coordinates and *t*-value of the peak value within each cluster. FA values within the following bilateral tracts are associated with word bias: arcuate fasciculas (arc), posterior limb of the internal capsule (pic), and posterior superior longitudinal fasciculus (pslf) (tract names determined using an interactive atlas linked here: http://dtiatlas.org/). Fig. 5 shows the location of each cluster projected onto the group mean FA skeleton (green) in relation to the SP network (blue).

2.3. Discussion

We hypothesized that individuals with a word bias would show enhanced structural integrity in brain areas associated with phonological and speech processing. Confirming our hypothesis, we found evidence that habitually attending to exogenous verbal information (i.e., word bias) is associated with increased white and grey matter volume in regions of modality congruent (verbal) cortex. Additionally, word bias was reflected in bilateral increases in connectivity along several major white matter tracts, including posterior superior longitudinal fasciculus, arcuate fasciculus and the posterior limb of the internal capsule. Remarkably, these regions partially overlap with a network derived from an *a priori* automated *meta*-analysis (NeuroSynth; Yarkoni et al., 2011) based on the search term "speech production." Relatedly, morphology within a large white matter volume adjacent to left insular cortex and spanning from left posterior frontal to left anterior and medial temporal regions, also positively covaried with word bias. Taken together, these results provide convergent evidence of long-term structural changes in left perisylvian linguistic regions of the brain associated with word bias. Thus, our results build upon prior functional neuroimaging research (Alfred et al., 2019; Kraemer et al., 2014, 2009), demonstrating a relationship between verbal HTs and

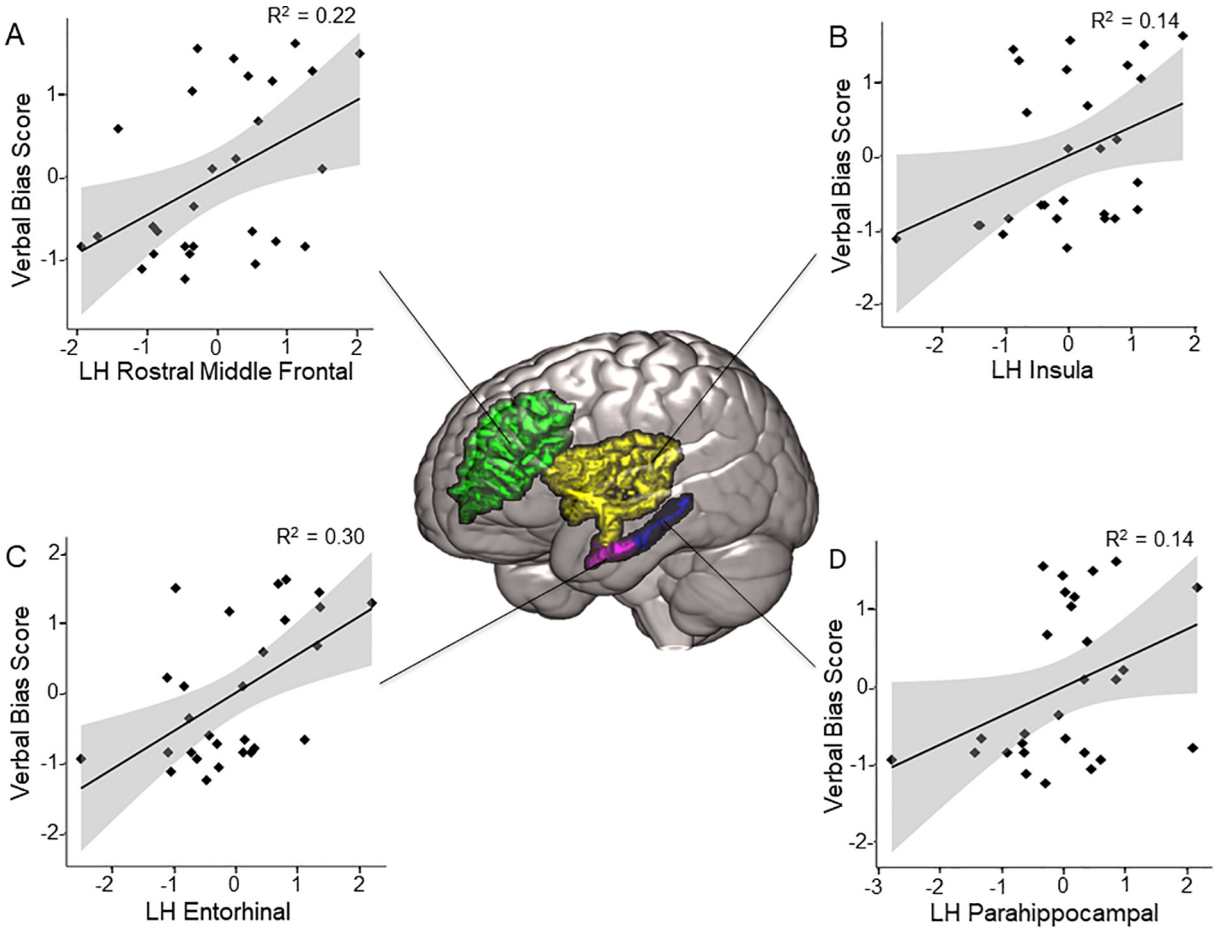

Fig. 4. Four white matter volume parcels (Desikan-Killiany Atlas) positively correlate with word bias scores: A) rostral middle-frontal, B) insula, C) entorhinal, and D) parahippocampal volumes. All data points were converted to z-values and Pearson's product-moment correlations are significant at the 0.05 alpha value after correcting for multiple comparisons (FDR).

persistent neuroanatomical changes observed in speech and phonological processing regions in the human brain.

In addition to those seen in left perisylvian regions, morphological differences in large-scale cortical and white matter structures associated with word bias were observed elsewhere in the brain. Several regions, including left entorhinal (ER) and right temporal pole areas (rTP), reflected associations with word bias in both grey and white matter (Note: white matter morphometry within rTP approached significance when compared with word bias scores [$r^2 = 0.14$; $p = 0.06$]). Entorhinal cortex (ERC) is involved in linking episodic memories to symbolic representations (written/spoken) while processing linguistic content (Goldinger, 2007; Meyer et al., 2005). Thus, one explanation for our results is that by preferentially attending to linguistic information, verbalizers persistently activate ERC in order to bind information from episodic memory to symbolic representations (i.e., words), resulting in enhanced structural integrity in this region. Similarly, the rTP also functions to integrate information from across the brain and has been described as a convergence zone (Damasio & Damasio, 1994), integrating distributed neural traces associated with disparate object properties into a cohesive, amodal representation (Coutanche & Thompson-Schill, 2015; Lambon et al., 2008; Lambon et al., 2009; Pobric et al., 2007; Visser et al., 2010). It is, therefore, likely that ERC and rTP contribute to converting multimodal neural traces into cohesive, linguistic representations.

It is worth mentioning that we are considering attentional bias as measured here as part of a broader construct, i.e., *habits of thought* (HTs) which subsumes *cognitive styles* and abilities. Cognitive style has traditionally been assessed using self-report assessments such as the visualizer-verbalizer questionnaire (VVQ; Kirby et al., 1988), which distinguishes individuals based on their preference for approaching content pertaining to either verbal or visuospatial formats. Although this construct has proven useful in distinguishing individuals in terms of

Table 1
White matter tracts associated with word bias scores. Included are the names of the major WM tract, the peak t-value and its location in MNI space, and the number of voxels within the cluster.

Major Fiber Tract	t-Max	Voxels (mm3)	t-Max X (mm)	t-Max Y (mm)	t-Max Z (mm)
LH Posterior Limb of Internal Capsule	2.98	141	−24	−14	9
LH Posterior Superior Longitudinal Fasciculus	3.74	141	−41	−28	31
LH Arcuate Fasciculus	3.66	114	−48	−37	−8
RH Posterior Limb of Internal Capsule	3.83	115	19	−13	−1
RH Posterior Superior Longitudinal Fasciculus	3.37	312	45	−17	35
RH Arcuate Fasciculus	3.03	110	49	−40	−5

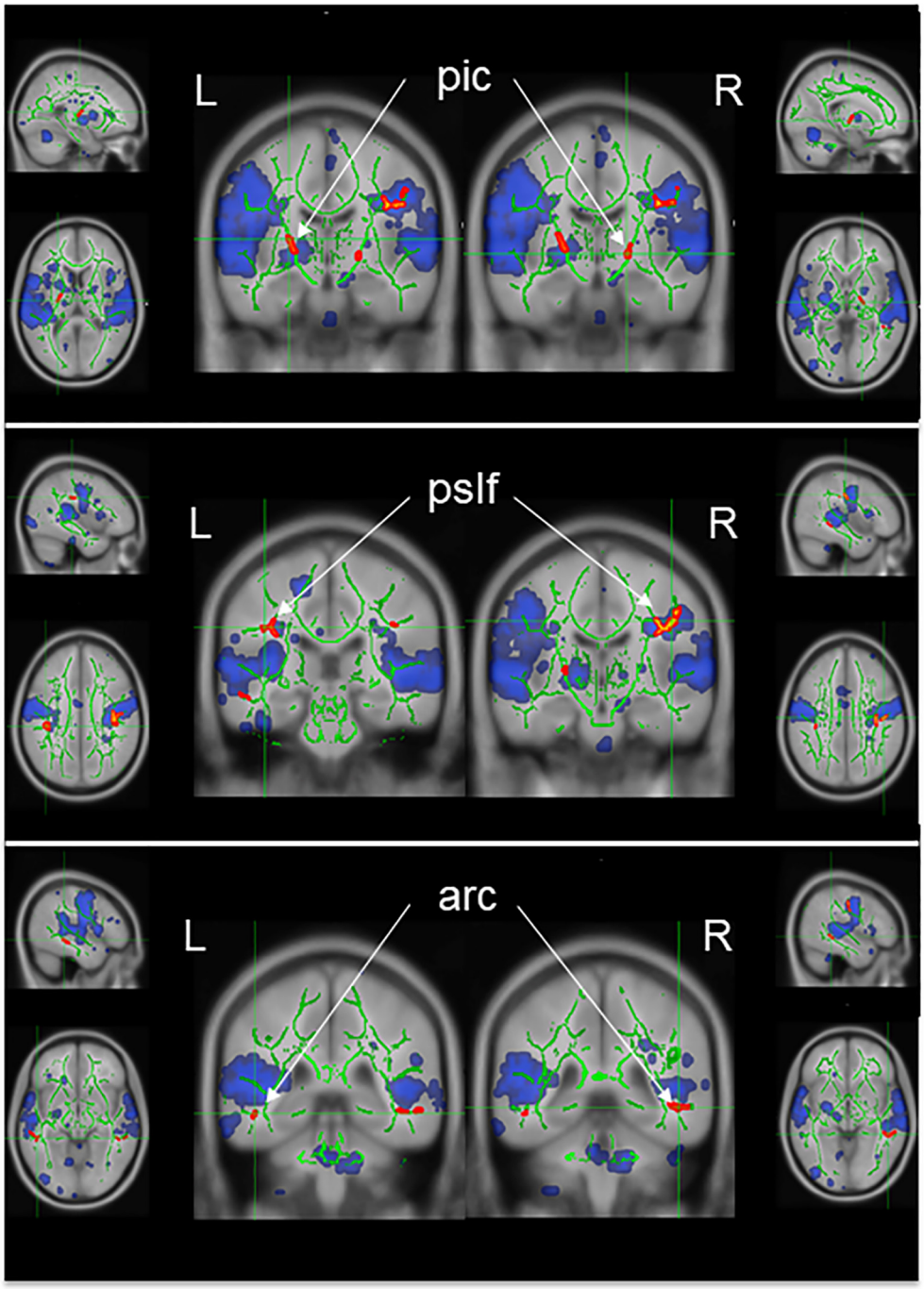

Fig. 5. White matter macrostructure within a bilateral *a priori* speech production network are associated with word bias. Crosshairs are centered over the peak voxel (see Table 1 for peak coordinates) within each cluster significantly correlated with word bias (shown in hot colors; expanded for visualization purposes). The speech production map is shown in blue. Shown in green is the group-wise mean FA skeleton. Major bilateral tracts shown include: A) posterior internal capsules (pic), B) posterior superior longitudinal fasciculi (pslf), and C) arcuate fasciculi (arc). All clusters shown are significant at the $p < 0.05$ level after permutation correction (1000 permutations) controlling for multiple comparisons.

subjective reports—we contend that a subjective report of preferences for visual or verbal content is limited, insofar as individuals' perceptions of their preferences may not match their habits. Thus, we designed the attentional bias (AB) task to measure an overlapping, albeit unique, construct pertaining to HTs. The AB task demands that individuals rapidly encode semantic information. By attending to words and thus, avoiding the need to convert pictorial stimuli into a linguistic representation (e.g., Kraemer et al., 2009), verbalizers would conserve metabolic resources during this task. In other words, the task was designed to assess automatic neurocognitive processing habits indicative of a habitual bias toward either verbal or visual information. Thus, with the AB task we hoped to capture an objective measure of HTs.

A limitation of the current work is our focus on the verbal end of the AB task. We chose to do this for several reasons. First, Blazhenkova and colleagues (2009) showed that the visual cognitive style is comprised of multiple dimensions—object and spatial imagery. With our limited sample size, we were concerned with being underpowered and thus, unable to find neural markers associated with a visual bias, given the noise introduced by having a sample containing object as well as spatial visualizers. Second, we hoped to extend the results of recent functional neuroimaging work (Alfred et al., 2019; Kraemer et al., 2014), focusing on verbal HTs, by demonstrating structural neural patterns associated with the construct. Nevertheless, a substantial neuroimaging literature reveals overlap between brain areas for perceiving and imagining visual objects (Chao & Martin, 1999; Cui et al., 2007; O'Craven & Kanwisher, 2000), and Kraemer and colleagues (2009) showed that visualizers translate verbal information into a visual format within the ventral processing stream. Thus, the current literature's focus on functional markers of visual HTs would benefit from future work exploring persistent anatomical features associated with the visual end of the

spectrum.

CRediT authorship contribution statement

Justin C. Hayes: Formal analysis, Writing - original draft, Visualization. **Katherine L. Alfred:** Investigation, Methodology, Data curation, Software, Writing - review & editing. **Rachel G. Pizzie:** Investigation, Data curation, Software, Writing - review & editing. **Joshua S. Cetron:** Investigation, Methodology, Software, Writing - review & editing. **David J.M. Kraemer:** Conceptualization, Methodology, Supervision, Project administration, Writing - review & editing.

Acknowledgements

The authors would like to thank the National Science Foundation (DRL-1661088 to DJMK) for funding this research. The authors would additionally like to thank Daniel J. Harris and Carissa A. Crawford for their contributions towards designing the Attentional Bias measure and collection of behavioral and neural data for this study.

References

Alfred, K. L., Hayes, J. C., Pizzie, R., Cetron, J. S., Kraemer, D. J. M. (2019). Individual differences in encoded neural representations within cortical speech production network [Preprint]. doi: 10.31234/osf.io/8wcpv.

Alloway, T.P., 2007. Automated Working Memory Assessment. Pearson Assessment, London.

Benjamini, Y., Hochberg, Y., 1995. Controlling the False Discovery Rate: A Practical and Powerful Approach to Multiple Testing. Retrieved from JSTOR.. J. R. Statist. Soc. Series B (Methodol.) 57 (1), 289–300.

Blazhenkova, O., Kozhevnikov, M., 2009. The new object-spatial-verbal cognitive style model: Theory and measurement. Appl. Cognit. Psychol. 23 (5), 638–663. https://doi.org/10.1002/acp.1473.

Chao, L.L., Martin, A., 1999. Cortical Regions Associated with Perceiving, Naming, and Knowing about Colors. J. Cognit. Neurosci. 11 (1), 25–35. https://doi.org/10.1162/089892999563229.

Coutanche, M.N., Thompson-Schill, S.L., 2015. Creating Concepts from Converging Features in Human Cortex. Cereb. Cortex 25 (9), 2584–2593. https://doi.org/10.1093/cercor/bhu057.

Cui, X., Jeter, C.B., Yang, D., Montague, P.R., Eagleman, D.M., 2007. Vividness of mental imagery: individual variability can be measured objectively. Vision Res. 47 (4), 474–478. https://doi.org/10.1016/j.visres.2006.11.013.

Damasio, A.R., Damasio, H., 1994. Cortical systems for retrieval of concrete knowledge: The convergence zone framework. In: Neuroscience, Computational (Ed.), Large-scale neuronal theories of the brain. The MIT Press, Cambridge, MA, US, pp. 61–74.

Desikan, R.S., Ségonne, F., Fischl, B., Quinn, B.T., Dickerson, B.C., Blacker, D., Killiany, R.J., 2006. An automated labeling system for subdividing the human cerebral cortex on MRI scans into gyral based regions of interest. NeuroImage 31 (3), 968–980. https://doi.org/10.1016/j.neuroimage.2006.01.021.

Fischl, B., Dale, A.M., 2000. Measuring the thickness of the human cerebral cortex from magnetic resonance images. PNAS 97 (20), 11050–11055. https://doi.org/10.1073/pnas.200033797.

Goldinger, S. D. (2007). A complementary-systems approach to abstract and episodic speech perception. Published in Proceedings of 2007 International Congress on Phonetic Sciences, 49–54.

Hsu, N.S., Kraemer, D.J.M., Oliver, R.T., Schlichting, M.L., Thompson-Schill, S.L., 2011. Color, context, and cognitive style: variations in color knowledge retrieval as a function of task and subject variables. J. Cognit. Neurosci. 23 (9), 2544–2557. https://doi.org/10.1162/jocn.2011.21619.

Jbabdi, S., Sotiropoulos, S.N., Savio, A.M., Graña, M., Behrens, T.E., 2012. Model-based analysis of multishell diffusion MR data for tractography: How to get over fitting problems. Magn. Reson. Med. 68 (6), 1846–1855.

Kirby, J.R., Moore, P.J., Schofield, N.J., 1988. Verbal and visual learning styles. Contemp. Educ. Psychol. 13 (2), 169–184. https://doi.org/10.1016/0361-476X(88)90017-3.

Kirchhoff, B.A., Buckner, R.L., 2006. Functional-anatomic correlates of individual differences in memory. Neuron 51 (2), 263–274. https://doi.org/10.1016/j.neuron.2006.06.006.

Kraemer, D.J.M., Hamilton, R.H., Messing, S.B., Desantis, J.H., Thompson-Schill, S.L., 2014. Cognitive style, cortical stimulation, and the conversion hypothesis. Front. Hum. Neurosci. 8, 15. https://doi.org/10.3389/fnhum.2014.00015.

Kraemer, D.J.M., Rosenberg, L.M., Thompson-Schill, S.L., 2009. The Neural Correlates of Visual and Verbal Cognitive Styles. J. Neurosci. Off. J. Soc. Neurosci. 29 (12), 3792–3798. https://doi.org/10.1523/JNEUROSCI.4635-08.2009.

Kubicki, M., McCarley, R., Westin, C.-F., Park, H.-J., Maier, S., Kikinis, R., Shenton, M.E., 2007. A review of diffusion tensor imaging studies in schizophrenia. J. Psychiatr. Res. 41 (1–2), 15–30. https://doi.org/10.1016/j.jpsychires.2005.05.005.

Lambon Ralph, M.A., Patterson, K., 2008. Generalization and differentiation in semantic memory: insights from semantic dementia. Ann. N. Y. Acad. Sci. 1124, 61–76. https://doi.org/10.1196/annals.1440.006.

Lambon Ralph, M.A., Pobric, G., Jefferies, E., 2009. Conceptual Knowledge Is Underpinned by the Temporal Pole Bilaterally: Convergent Evidence from rTMS. Cereb. Cortex 19 (4), 832–838. https://doi.org/10.1093/cercor/bhn131.

Lowe, M.J., Beall, E.B., Sakaie, K.E., Koenig, K.A., Stone, L., Marrie, R.A., Phillips, M.D., 2008. Resting state sensorimotor functional connectivity in multiple sclerosis inversely correlates with transcallosal motor pathway transverse diffusivity. Hum. Brain Mapp. 29 (7), 818–827. https://doi.org/10.1002/hbm.20576.

Messick, S., et al. (1976). Individuality in learning. Oxford, England: Jossey-Bass.

Meyer, P., Mecklinger, A., Grunwald, T., Fell, J., Elger, C.E., Friederici, A.D., 2005. Language processing within the human medial temporal lobe. Hippocampus 15 (4), 451–459. https://doi.org/10.1002/hipo.20070.

Miller, M.B., Donovan, C.-L., Bennett, C.M., Aminoff, E.M., Mayer, R.E., 2012. Individual differences in cognitive style and strategy predict similarities in the patterns of brain activity between individuals. NeuroImage 59 (1), 83–93. https://doi.org/10.1016/j.neuroimage.2011.05.060.

Miller, M.B., Donovan, C.-L., Van Horn, J.D., German, E., Sokol-Hessner, P., Wolford, G.L., 2009. Unique and persistent individual patterns of brain activity across different memory retrieval tasks. NeuroImage 48 (3), 625–635. https://doi.org/10.1016/j.neuroimage.2009.06.033.

O'Craven, K.M., Kanwisher, N., 2000. Mental Imagery of Faces and Places Activates Corresponding Stimulus-Specific Brain Regions. J. Cognit. Neurosci. 12 (6), 1013–1023. https://doi.org/10.1162/08989290051137549.

Pobric, G., Jefferies, E., Ralph, M.A.L., 2007. Anterior temporal lobes mediate semantic representation: Mimicking semantic dementia by using rTMS in normal participants. Proc. Natl. Acad. Sci. 104 (50), 20137–20141. https://doi.org/10.1073/pnas.0707383104.

Sahyoun, C.P., Belliveau, J.W., Mody, M., 2010a. White matter integrity and pictorial reasoning in high-functioning children with autism. Brain Cogn. 73 (3), 180–188. https://doi.org/10.1016/j.bandc.2010.05.002.

Sahyoun, C.P., Belliveau, J.W., Soulières, I., Schwartz, S., Mody, M., 2010b. Neuroimaging of the Functional and Structural Networks Underlying Visuospatial versus Linguistic Reasoning in High-Functioning Autism. Neuropsychologia 48 (1), 86–95. https://doi.org/10.1016/j.neuropsychologia.2009.08.013.

Smith, S.M., Jenkinson, M., Johansen-Berg, H., Rueckert, D., Nichols, T.E., Mackay, C.E., Behrens, T.E.J., 2006. Tract-based spatial statistics: Voxelwise analysis of multi-subject diffusion data. NeuroImage 31 (4), 1487–1505. https://doi.org/10.1016/j.neuroimage.2006.02.024.

Smith, S.M., Jenkinson, M., Woolrich, M.W., Beckmann, C.F., Behrens, T.E.J., Johansen-Berg, H., Matthews, P.M., 2004. Advances in functional and structural MR image analysis and implementation as FSL. NeuroImage 23 (Suppl 1), S208–219. https://doi.org/10.1016/j.neuroimage.2004.07.051.

Smith, S.M., Nichols, T.E., 2009. Threshold-free cluster enhancement: addressing problems of smoothing, threshold dependence and localisation in cluster inference. NeuroImage 44 (1), 83–98. https://doi.org/10.1016/j.neuroimage.2008.03.061.

Soares, J.M., Marques, P., Alves, V., Sousa, N., 2013. A hitchhiker's guide to diffusion tensor imaging. Front. Neurosci. 7. https://doi.org/10.3389/fnins.2013.00031.

Tessitore, A., Giordano, A., Russo, A., Tedeschi, G., 2016. Structural connectivity in Parkinson's disease. Parkinson. Relat. Disord. 22 (Suppl 1), S56–59. https://doi.org/10.1016/j.parkreldis.2015.09.018.

Visser, M., Embleton, K.V., Jefferies, E., Parker, G.J., Ralph, M.A.L., 2010. The inferior, anterior temporal lobes and semantic memory clarified: novel evidence from distortion-corrected fMRI. Neuropsychologia 48 (6), 1689–1696. https://doi.org/10.1016/j.neuropsychologia.2010.02.016.

Wechsler, D., 1999. Wechsler Abbreviated Scale of Intelligence. The Psychological Corporation, San Antonio, TX.

Winkler, A.M., Ridgway, G.R., Webster, M.A., Smith, S.M., Nichols, T.E., 2014. Permutation inference for the general linear model. NeuroImage 92, 381–397. https://doi.org/10.1016/j.neuroimage.2014.01.060.

Yarkoni, T., Poldrack, R.A., Nichols, T.E., Van Essen, D.C., Wager, T.D., 2011. Large-scale automated synthesis of human functional neuroimaging data. Nat. Methods 8 (8), 665–670. https://doi.org/10.1038/nmeth.1635.